Effect of casein/whey ratio on the thermal denaturation of whey proteins and subsequent fouling in a plate heat exchanger

Weiji Liu, Xiao Dong Chen, Romain Jeantet, Christophe André, Séverine Bellayer, Guillaume Delaplace

Effect of casein/whey ratio on the thermal denaturation of whey proteins and subsequent fouling in a plate heat exchanger

Weiji Liu [a,b,e,*], Xiao Dong Chen [a,e], Romain Jeantet [c,e], Christophe André [d], Severine Bellayer [e], Guillaume Delaplace [b,e]

[a] School of Chemical and Environmental Engineering, Soochow University, Suzhou, Jiangsu, 215123, PR China
[b] Univ. Lille, CNRS, INRAE, Centrale Lille, UMR 8207 - UMET - Unité Matériaux et Transformations, F-59000, Lille, France
[c] STLO, INRAE, Institut Agro, 35042, Rennes, France
[d] HEI (Ecole des Hautes Etudes d'Ingénieur), Départment Chimie, Textiles et Process Innovants, 13, rue de Toul, 59046, Lille, Cedex, France
[e] International Joint Laboratory (INRAE Villeneuve d'Ascq-Soochow University-Agrocampus Rennes), School of Chemical and Environmental Engineering, College of Chemistry, Chemical Engineering and Materials Science, Soochow University, Suzhou, Jiangsu, 215123, PR China

ARTICLE INFO

ABSTRACT

Dairy fouling is a ubiquitous problem in food processing, however, the fouling mechanism is not fully understood and investigations arose mainly from experiments with model systems that contained only whey proteins, typically reconstituted from whey protein isolate powder (WPI). The effect of casein on fouling has been rarely considered despite it is the major component of milk proteins. To fill this gap, whey protein-based model fluids containing different casein concentrations and fixed content of added calcium were prepared, leading to various Casein/WPI mass ratios. The effect of Casein/WPI on β-lactoglobulin (BLG) denaturation at molecular level and subsequent fouling behavior in the pilot-scale plate heat exchanger during pasteurization treatment was investigated. It was shown that Casein/WPI significantly affects the fouling behavior: at low Casein/WPI, fouling mass dropped dramatically until a minimum value was reached located at Casein/WPI of 0.2. While at higher Casein/WPI, fouling mass increased with elevated Casein/WPI. Element mapping of the fouling layer also reveals that different structures and fouling mechanisms occur depending on Casein/WPI ratio. Finally, it was established that contrary to WPI solutions, BLG thermal denaturation is poorly correlated to decrease/extent of fouling for casein protein-based solutions showing that the presence of casein deeply modifies mineral and protein interactions and fouling build-up.

1. Introduction

Milk fouling upon plate heat exchanger (PHE) is a ubiquitous problem in the manufacturing processes of dairy factories as in the case of pasteurization, giving negative impacts on operating costs and product quality. It is responsible for several industrial issues, such as reduction of heat transfer efficiency (Mahdi et al., 2009), pressure-drop (Grijspeerdt et al., 2004), and also increasing risk of microbial contamination (Fryer et al., 2006). Another serious problem associated with fouling is the cleaning process for fouled surfaces, where environmentally offensive chemicals are usually employed.

Given these negative impacts of fouling in PHE, tremendous efforts have been paid to explore the mechanism lying behind. The overview of the fouling mechanism has been systematically addressed as reviewed by Sadeghinezhad et al. (2015) and Bansal and Chen (2006). Two dominant mechanisms are recognized for milk-based fouling named i) heat-induced denaturation of protein and ii) mineral precipitations. β-lactoglobulin (BLG) is the major protein responsible for the protein fouling due to its exposed thiol group after thermal denaturation and thus initializes the protein interaction through SH/S–S interchange reactions (Shimada and Cheftel, 2002).

Despite the comprehensive mechanism discovered in the literature, the role of casein proteins on fouling is not yet fully understood, the main reason being that the fouling phenomenon was most studied for whey protein solutions which are casein free. Unfortunately, the presence of individual caseins or micellar casein complicates seriously the mechanisms concerning both the protein denaturation and mineral precipitations. In the aspect of protein denaturation, the most frequently

---

mentioned in the literature is the interaction between κ-casein and de-natured BLG. It was proposed that denatured BLG can either interact with κ-casein on the surface of casein micelle or in the serum phase after being dissociated from the micellar structure (Wijayanti et al., 2014). Besides that, casein has been reported to have chaperone functions on the thermal denaturation of whey proteins. The BLG-initiated poly-merization is disrupted due to the association between casein and de-natured whey proteins probably through hydrophobic interactions (Bhattacharyya and Das, 1999; Morgan et al., 2005). Additionally, casein can affect the mineral balances in the milk, particularly, transfer the ionic calcium into micellar calcium phosphate upon heating (On-Nom et al., 2010; Udabage et al., 2000). Nevertheless, the exact role of micellar casein on fouling is still far away from clear.

A study of how casein affects the thermal denaturation kinetics of whey proteins could lead to a better understanding of the relationship between casein and whey protein under heat treatment. Indeed, there are numerous reports of kinetics studies on the thermal denaturation of major whey proteins (Anema and McKenna, 1996; Dannenberg and Kessler, 1988; Hillier and Lyster, 1979; Oldfield et al., 1998; Park and Lund, 1984; Sawyer et al., 1971), while few of them focused on the effect of casein. And if the effect of casein on fouling is desired, different proportions of casein/whey should be concerned (Kessler and Beyer, 1991; Patocka et al., 1993). In this paper, reconstituted whey protein isolate (WPI) solutions at 0.5 wt% with various casein protein concen-trations to have different Casein/WPI proportions were used as model fluids. An appropriate amount of calcium chloride was also added in order to provide a suitable level of calcium for fouling to occur. The free Ca^{2+} concentrations used in this study are close to that observed in milk at ~80–170 mg/L (Lewis, 2011). The fouling experiments were carried out in a pilot-scale PHE for a given thermal profile. The mass of fouling deposits and the pressure-drop evolution in the PHE was recorded; the morphology and chemical compositions of the fouling layer were also investigated using Electron Probe Micro Analyzer (EPMA) and gel-electrophoresis, respectively. In addition, the effect of casein on molecular scale was also evaluated through the thermal denaturation kinetics of BLG using a one-step reaction model.

2. Materials and methods

2.1. Model fouling solutions

The fouling solutions used in this study were reconstituted from PRODIET 90 S WPI powder and PRODIET 87 B casein powder supplied by Ingredia (France). According to the manufacturer, WPI powder consists of 85.5 wt% total protein, 5.5 wt% moisture, 0.2 wt% calcium and phosphorous. The casein powder contains 83 wt% total protein, 5 wt% moisture, 2.6 wt% calcium and 1.3 wt% phosphorous. For all exper-imental solutions, the whey protein concentration was fixed at 0.5 wt% to simulate the whey protein content in raw milk (Farrell et al., 2004). In order to investigate the effect of casein on the fouling behavior, different amount of casein powder was added to achieved elevated Casein/WPI mass ratio from 0 to 0.8. Preliminary experiments showed no visible fouling when using WPI alone or mixtures of WPI and casein (Casein/-WPI mass ratio up to 1). Therefore, it was decided to add 42 ppm of free calcium in the form of calcium chloride (anhydrous, 96%, Acros Or-ganics, USA) in the fouling solutions. $CaCl_2$ has been widely used in the literature to introduce calcium ios into dairy systems, and is authorized sicnce ages to be added to milk during cheece making (Price, 1927). The amount of $CaCl_2$ was determined to achieve a suitable total fouling mass in the PHE. The total amount of calcium is similar to those used for WPI fouling experiments (Guérin et al., 2007; Khaldi et al., 2015, 2018).

2.2. Pilot-scale fouling runs

Fouling experiments were performed on the pilot-scale set-up as shown in Fig. 1. The system contained two PHEs (Model V7, Alfa-Laval

Vicard, France); they were both configured using 21 plates thus proving 10 channels for both hot water and fouling fluid. The dimension of the plate is 150 mm × 495 mm × 0.8 mm with a corrugated surface (35° corrugation angle with a 3.9 mm flow gap), giving an effective contact area of 0.0743 m². The first PHE is named pre-heating PHE as it allows to increase the temperature of fouling solutions from 50 to 65 °C without inducing denaturation of BLG and fouling (Boye and Alli, 2000). The main fouling observations were focused on the second PHE, called heating PHE, which continues elevating the solutions up to 85 °C at its outlet; this temperature was kept constant by controlling the inlet of hot water, thereby a constant temperature profile along the PHE was ach-ieved. A quasi-linear temperature profile with PHE was obtained in a counter-current configuration of fouling fluid and hot water with the same flow rate at 300 L·h⁻¹ (See Supplementary Information Fig. S1), the bulk temperature profile was simulated numerically using Sphere software (Fig. S2) which was previously elaborated and validated by INRA's group as mentioned in Blanpain-Avet et al. (2016) and Petit et al. (2013). This temperature profile resembles an HTST (High Temperature Short Time) pasteurization process with slightly higher temperature and duration. The temperature and flow rate measurements were performed using platinum resistance probes (Pt100, Fer Constantan) and electro-magnetic flowmeters (Krohene IFM, Germany), respectively. All sensors were calibrated before the experiments were conducted; the accuracy of temperature measurements was expected to be better than ±0.2 °C and relative errors for the flow rate measurements were considered to be less than ±1%. All measurements were collected using a data acquisition system (Agilent Technologies 34970A, USA).

Prior to fouling runs, the fouling solutions were stirred in a 750 L tank; the temperature of the solutions was increased to 50 °C and maintained for at least 1 h to ensure full dissolution of protein powders. Before pumping fouling fluid, reverse osmosis water was firstly used to reach a thermal equilibrium of the system at the desired process tem-perature. After that, 600 L of fouling solution was processed in each pilot-scale experiment by switching from water to fouling fluid once-through, without recycling. This volume corresponds to a total running time of 2 h, during which the fouling solutions were sampled at both inlet and outlet of the heating PHE three times; these solutions along with the solution in the launching tank (i.e. fouling solution at 50 °C) were used for subsequent determination including pH, free calcium content, total calcium content, and BLG denaturation. To quickly quench the denaturation of proteins in sample solutions, they were mixed immediately with cold water (<1 °C) in a centrifugation tube. The dilution effect was considered in the calculation of calcium and protein concentration. When the fouling experiments were finished, water was used again to replace fouling solutions in the channels; after that, the PHE was dismantled and placed under ambient conditions overnight before putting in an air-oven at 50 °C for at least 3 h to dry the plates. The dry mass of the fouling deposit on each plate was calculated by the difference between bare and fouled plates. Fouling mass in each channel was the addition of two deposit mass values obtained for the plates constituting the pass walls. The total fouling mass for each run is the sum of the mass collected from all the channels.

Finally, these plates were installed again in the PHE system for the subsequent cleaning procedure by circulating 2 wt% sodium hydroxide (99%, Solvay, Belgium) and 2 wt% nitric acid (54%, Thermo Fisher Scientific) with a similar heating process to the fouling experiments. The duration for each step lasted at least 30 min, after that, the system was rinsed with osmosis water for the next heat treatment experiment. The cleanliness of the plates was check visually to ensure efficient cleaning.

The amount of fouling was also monitored by the pressure-drop within PHE and the calculation of thermal resistance (Rf). Assuming uniform fouling layer, the average thermal resistance Rf can be described as:

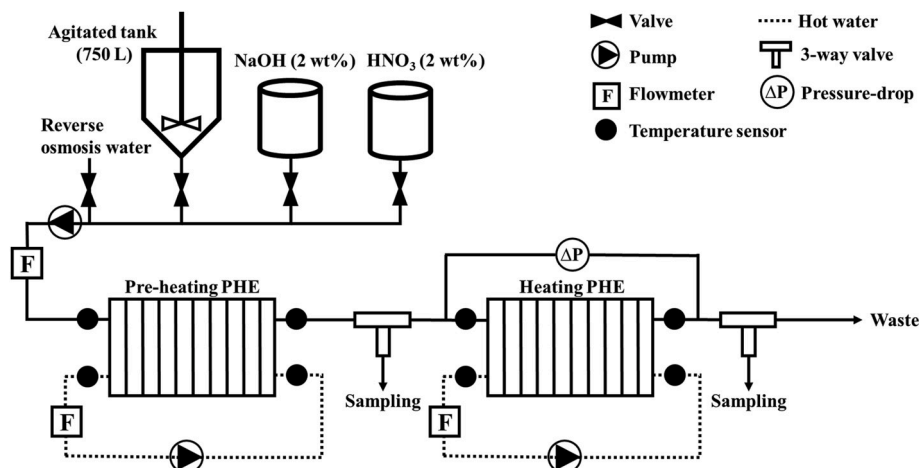$$Rf = \frac{1}{Ut} - \frac{1}{U0} \qquad (1)$$

Fig. 1. Schematic diagram of pilot-scale fouling experimental set-up. Two plate heat exchangers (PHEs) were coupled and named pre-heating PHE and hearting PHE, respectively.

where $U0$ and Ut are the overall heat transfer coefficients before the occurrence of fouling and at time t when fouling is formed, respectively.

The heat transfer coefficient was calculated from the energy balance between the heating fluid (hot water) and processed fluid (model solution):

$$mhCph(Th,i - Th,o) = US\Delta TLMTD \qquad (2)$$

where mh and Cph represents the mass flow rate (kg·s^{-1}) and the specific heat for the hot water (J·kg^{-1}·K^{-1}), respectively. The temperature dependence of Cph was used as reported by Petit et al. (2013). Th,i and Th,o refers to the temperature of hot water at the inlet and outlet of PHE (K). S is the heat transfer area (m^2), and $\Delta TLMTD$ is the logarithmic mean temperature difference (K).

2.3. Calcium content measurement

The ionic or free calcium [Ca]$_f$ of sample solutions was measured using a calcium ion-selective electrode (Ca-ISE, PS-3518, PASCO, USA). The calculation of the free calcium level was based on the potential difference between the sample solution and a constant reference through a gelled organophilic membrane. The potential values were recorded in the software from the manufacturer (PASCO capstone) through a Bluetooth module coupled with the electrode. A high and constant ionic strength environment was needed for reliable potential measurements, hence 3.85% (v/v) of the ionic strength adjuster (4M KCl) was added for all samples and standard solutions. The probe was calibrated with five Ca^{2+} standards ranging from 5 ppm to 100 ppm. The calibration curve was derived from the logarithm of Ca^{2+} concentration and the potential values according to the Nernst equation. To avoid any temperature effect, all samples and standard solutions were allowed to equilibria in a 25 °C water bath for at least 1 h before measurements. The total calcium content [Ca]$_t$ was determined by atomic absorption spectrometry using a Spectro AA 55B apparatus (Varian, Palo Alto, USA) as performed in Khaldi et al. (2018).

2.4. High-performance liquid chromatography

The concentration of soluble BLG in the samples was evaluated using a high-performance liquid chromatography (HPLC) system (Alliance HPLC System, Waters, USA). The chromatographic system consists of a separation module integrated solvent and sample management functions (e2695 Separation Module), a column heater/cooler, a reverse-phase column (XBridge Protein BEH C4, 300 Å, 3.5 μm, Waters) associated with a guard column (Sentry Guard Cartridge, Waters), a UV–Vis

spectrophotometer (2998 PDA Detector) and acquisition software (Empower Software).

The pH of the protein samples was adjusted to 4.6 following a centrifugation process (9056×g for 30 min at 4 °C) to remove aggregated BLG and casein proteins if any. The supernatants were filtered through a 0.2 μm cellulose filter (Minisart RC, Sartorius, Germany) before injecting 20 μL in the HPLC system. Two mobile phases were used: solution A consists of 0.1% (v/v) trifluoroacetic acid (TFA, 99%, Acros Organics) in MilliQ water while solution B contains 0.1% (v/v) TFA, 80% acetonitrile (HPLC grade, Thermo Fisher Scientific) and 20% MilliQ. The separation was performed at a flow rate of 1 mL/min, 40 °C and a detection wavelength of 215 nm with gradient elution. Calibration curves were done by using pure BLG standards (0.25–3 g/L). To maintain the performance of the column, pure acetonitrile was eluted at 1 mL/min for 1 h after the experiment finished.

2.5. Characterization of the fouling deposit

To provide a deeper insight into the fouling, the determination of element and protein composition was carried out using an Electron Probe Micro Analyzer (EPMA) and Sodium Dodecyl Sulfate Poly-acrylamide Gel Electrophoresis (SDS-PAGE), respectively. The characterizations were performed for the fouling runs at four different Casein/WPI mass ratios at 0, 0.05, 0.2 and 0.8, and for each experiment, the deposits formed at two different plates were studied for comparison purposes (*i.e.* P$_{14}$ and P$_{21}$, Fig. S1).

For EPMA analysis, the samples were directly cut from the dried plate after the fouling experiments, the analyzed deposits were chosen on the flat surface of the plate. The corresponding bulk temperatures are 78.9 and 84.6 °C for samples collected from P$_{14}$ and P$_{21}$, respectively (Fig. S2). The cut coupons were firstly embedded in epoxy resin; after solidification, the surface was polished using an ESC 200 GT polishing machine (ESCIL, Chassieu, France) with different grades of SiC sheets (up to 0.25 μm) and carbon coated with a Bal-Tec SCD005 sputter coater. These processes are necessary to ensure a very flat surface for EPMA measurement. The samples were placed in the vacuum and excited by an electron beam, the backscattered electron imaging and X-ray mapping were carried out using a Cameca SX-100 EPMA (CAMECA, Gennevilliers, France) at 15 kV, 15 nA, and 15 kV, 40 nA, respectively. For element determination, a PET crystal was used to detect Kα X-rays of sulfur, calcium, and phosphate, and a LiF crystal to detect iron Kα X-rays.

The SDS-PAGE was performed in a SE 600 Series vertical Slab Gel Unit (Hoefer Scientific instrument, San Francisco, US). The resolving gel contained 15% (w/v) acrylamide and 0.2% (w/v) SDS in 1.5 M Tris-HCl

buffer at pH 8.8, and the stacking gel included 4% (w/v) acrylamide and 0.1% (w/v) SDS in 0.5 M Tris-HCl buffer at pH 6.8. The deposit samples were scraped from the dried plate after the fouling runs and dried again in a 105 °C oven for over 24 h. The dry powders were ground and dissolved in the sampling buffer (0.5 M Tris-HCl buffer, pH 6.8, containing 0.2% (w/v) SDS, 0.01% (v/v) bromophenol blue and 0.05% (v/v) β-mercaptoethanol) with a final concentration at 0.5 wt%. Pure proteins including α/β/κ-casein, αLa, BSA and BLG were also dispersed in the sampling buffer for a comparison purpose. These solutions were heated in a boiling water bath for 5 min; they were cooled to room temperature and injected into the gel along with a protein molecular weight ladder (Precision Plus Protein Unstained Standards, Bio-Rad Laboratories, UK). The gels were run under a constant current at 40 mA for immigration in the stacking gel and 60 mA for resolving gel. After electrophoresis, a fixation process was applied by immersing the gel in the solution with 10% (v/v) acetic acid (99.5%, Acros Organics) and 30% (v/v) ethanol. After that, the gel was stained for at least 2 h using 0.02% (m/v) Brilliant Blue R in 10% (v/v) acetic acid and 25% (v/v) isopropanol. After coloration, the gel was destained using a 10% (v/v) acetic acid solution until a clear background was achieved.

2.6. Thermal denaturation experiments

The model solutions for denaturation experiments were selected according to the pilot-scale fouling results: 0.5 wt% WPI, 0.5 wt% WPI with 0.25 wt% casein, 0.5 wt% WPI with additional 42 ppm free calcium at different Casein/WPI mass ratio of 0, 0.05, 0.2 and 0.8, respectively. The compositions of these solutions were summarized in Table 1. The experimental protocol was similar as reported previously by Petit et al. (2011). Briefly, all model solutions were reconstituted using a similar protocol as applied in the fouling experiments (*i.e.* 50 °C for 3 h), after that 2 mL aliquots were removed into plastic tubes (Eppendorf, Germany) prior to heat treatment. The heating process included three stages by using three water baths: the first water bath was set at 65 °C to pre-heat the solutions below the critical temperature for BLG denaturation (Paulsson and Dejmek, 1990), and the second bath was set at 10 °C higher than the desired holding temperature (T_d+10 °C) to quickly heat up the solution to reach T_d, at which it corresponded to time zero for kinetic calculation. After that, the samples were maintained at T_d by submitting into the third bath (temperature set at T_d+1 °C). The sample temperature was monitored by following the temperature evolution of a reference vial filled with the MilliQ, in which a thermocouple was inserted. The holding temperature T_d varied from 70 to 90 °C was maintained for a proper period of time to induce significant BLG denaturation. At different times (including solution reach 65 °C in the first bath), the solutions were removed and cooled in melting ice to quench the BLG denaturation.

2.7. BLG denaturation using one-step reaction model

The thermal denaturation of BLG is widely accepted in a multi-stages mechanism (Tolkach and Kulozik, 2007). Despite this intricate mechanism, the denaturation pathway of BLG is generally simplified due to the lack of ability to distinguish different BLG monomers (*e.g.* native and

unfolded), for example when using polarimetric analysis (Ven Murthy and Carrier-Malhotra, 1989), gel permeation chromatography (Kehoe et al., 2011), immunodiffusion (Miyawaki et al., 2003), electrophoresis (Oldfield et al., 2005), or reverse-phase high performance liquid chromatography (RP-HPLC) (Khaldi et al., 2015; Petit et al., 2011). In the HPLC system, the determined BLG consists of both native and unfolded BLG molecules, which is also called soluble BLG. Hence, an overall one-step model was established by considering the transformation of soluble species (S) into aggregated ones (A). The reaction rate of this chemical reaction can be described as:

$$-\frac{dC_s}{dt} = k_f C_s^n \tag{3}$$

where C_s refers to the concentration of soluble BLG species as determined in the HPLC system, and k_f is the denaturation rate constant. The unit of k_f depends on the reaction order n (*i.e.* $g^{1-n} \cdot L^{n-1} \cdot s^{-1}$). The experimental data were fitted to equation (1) using Matlab to calculate the denaturation rate constant k_f with various reaction order from 1 to 3. The reaction order was determined according to the RSS values (Residual sum of squares) obtained by fitting equation (1) to the experimental data (Fig. S3), where the most suitable values were found to be 2. This value is consistent with those found for BLG denaturation in skim milk (Hillier and Lyster, 1979; Lyster, 1970; Manji and Kakuda, 1986) or simulated milk ultrafiltrate (Park and Lund, 1984).

2.8. Temperature dependence of k_f

The relationship between k_f and the heating temperature is deduced by the Arrhenius equation:

$$\ln(kn) = \ln(k0) - \frac{Ea}{RT} \tag{4}$$

where k0 is the denaturation frequency factor ($g^{1-n} \cdot L^{n-1} \cdot s^{-1}$), Ea is the activation energy ($J \cdot mol^{-1}$), R is the universal gas constant ($J \cdot mol^{-1} \cdot K^{-1}$), and T is the bulk liquid temperature (K).

Fig. 2 presents an example of Arrhenius plot obtained from a solution containing 0.5 wt% WPI with the addition of 42 ppm Ca^{2+}, where the logarithm of k_f is plotted against the inverse temperature. A break of the slope appears around a critical temperature (T_c, *i.e.* 82 °C in this case) as previously observed and interpreted by Tolkach and Kulozik (2007) is unexpected for a one-step reaction as described from equation (2), hence it is generally deduced with a two-step reaction mechanism:

$$N \rightarrow U \rightarrow A \tag{5}$$

where the native BLG molecule (N) unfolds (U) prior to forming aggregates (A). At temperatures lower than the critical temperature T_c, the unfolding reaction rate is considered to be lower than the aggregation while when the temperature is higher than T_c, the unfolding rate is faster. Consequently, linear regressions of data at these two regions permit us to determine the kinetic parameters, including k_0 and Ea, for both unfolding and aggregation steps.

Table 1
Composition of model solutions for thermal denaturation experiments.

Solutions	[WPI] (wt%)	[Casein] (wt%)	[Casein]/[WPI]	Added Ca^{2+} (ppm)	[Ca]$_f$[a] (ppm)	[Ca]$_t$[b] (ppm)
Casein/WPI = 0	0.5	0	0	0	14.7	22.3
Casein/WPI = 0.5	0.5	0.25	0.5	0	58.1	91.0
Casein/WPI = 0&Ca	0.5	0	0	42	53.1	64.7
Casein/WPI = 0.05&Ca	0.5	0.025	0.05	42	61.2	74.3
Casein/WPI = 0.2&Ca	0.5	0.1	0.2	42	67.9	90.9
Casein/WPI = 0.8&Ca	0.5	0.4	0.8	42	96.2	169.4

[a] Free calcium concentration determined using Ca-ISE.
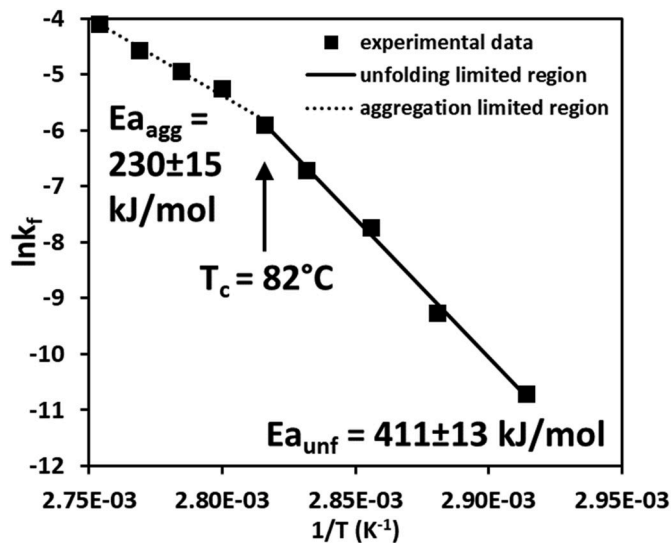[b] total calcium concentration obtained from AAS.

Fig. 2. Arrhenius plot of 0.5 wt% WPI solutions with the addition of 42 ppm Ca^{2+}. The solution contains 53 ppm Ca^{2+} with 64.7 ppm total Ca. The denaturation reaction rate k_f was obtained by solving equation (1) with a reaction order of 2.

Fig. 3. Effect of $[Ca]_t$/BLG ratio on the total dried fouling mass of 0.5 wt% WPI. The symbols in triangles refer to the data reported in Khaldi, Croguennec, André, Ronse, Jimenez, Bellayer, Blanpain-Avet, Bouvier, Six, Bornaz, Jeantet and Dclaplacc (18). Solid line presents linear regression with a value of R^2 at 0.994.

3. Results and discussion

3.1. The essential role of Ca^{2+} on fouling

It is important to bear in mind that introducing casein powder can also bring additional minerals to the system, in particular, calcium on ionic and colloidal forms. It was decided to first investigate the effect of Ca^{2+} on the mass of whey protein fouling deposits formed inside PHE. Table 2 summarizes the calcium compositions of nine different fouling fluids and their corresponding fouling results, including BLG concentrations at the inlet and outlet of PHE, BLG denaturation level within PHE, and total fouling mass.

The solution containing whey proteins alone was incapable to induce detectable fouling deposits under our operating conditions due to its minor content of calcium (22 ppm of total calcium with ~15 ppm ionic calcium). However, if Ca^{2+} was added to increase the level of free calcium (in the form of $CaCl_2$), fouling deposits were obtained. As shown in Fig. 3, the total amount of dried fouling deposits increase at elevated Ca/BLG ratio in a linear pattern ($R^2 = 0.994$). This effect of ionic calcium on fouling mass has been proved previously by Guérin et al. (2007), Khaldi et al. (2015) and Khaldi et al. (2018) for other aqueous solutions reconstituted from different WPI powders and heat-treated with similar
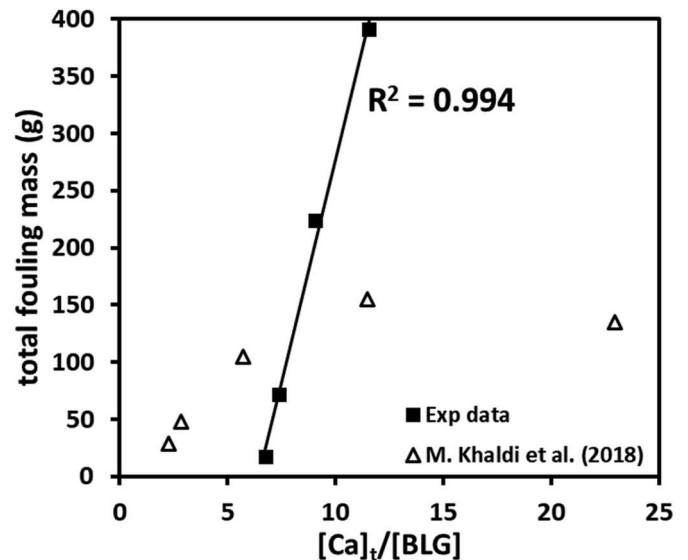
thermal schedule. For example, Khaldi et al. (2018) have investigated the effect of Ca/BLG on whey protein fouling and pointed out that Ca/BLG ratio alters the structure of the fouling layer, and observed more surprisingly, that for the range of Ca/BLG ratios investigated (2.3–22.9), the fouling mass is dependent on this ratio and not driven by the protein concentration as commonly admitted. Their data are also presented in the figure for comparison while a plateau is reached in their case, which might due to the lower protein concentration they used at higher Ca/BLG ratio. Another significant impact of Ca/BLG on fouling behavior can be found on the BLG denaturation level within PHE. For example, the BLG denaturation level is only 7.7% without additional Ca^{2+}, but the values increase up to 44.5% for the case where 390.8 g of fouling mass was obtained (close to the operating limitation). One might notice that the increased extent of BLG denaturation level is relatively lower than the increased fouling mass evolution at higher Ca/BLG ratio, suggesting that calcium could be a foulant intermediate facilitating the fouling growth and not only involved in the extent of protein denaturation.

Knowing the effect of Ca^{2+} on fouling, an appropriate amount of casein was added instead of $CaCl_2$ attempting to achieve a similar Ca^{2+} level (Fluid#6, #7 compared to #4 and #5). Surprisingly, despite the high concentration of ionic calcium or even much more total calcium

Table 2

Calcium content of nine different fouling fluids and their corresponding fouling results. For each fouling experiment, the BLG concentration at the inlet and outlet of PHE are also shown. Errors represent standard deviation (SD).

Fluid#	Casein/WPI	Added Ca^{2+} (ppm)	$[Ca]_f$[a] (ppm)	$[Ca]_t$[a] (ppm)	$[BLG]_{inlet}$[b] (g/L)	$[BLG]_{outlet}$[c] (g/L)	BLG denaturation level[d]	Total fouling mass (g)
#1	0	0	14.8 ± 0.6	22.3 ± 1.2	3.08 ± 0.04	2.84 ± 0.05	7.7%	N/A[e]
#2	0	25	38.7 ± 0.7	48.4 ± 1.9	3.30 ± 0.02	2.40 ± 0.09	27.2%	17.1
#3	0	35	37.5 ± 1.6	59.4 ± 1.8	3.55 ± 0.15	2.1 ± 0.4	40.8%	72.1
#4	0	42	53.0 ± 1.9	64.7 ± 2.6	3.28 ± 0.06	1.87 ± 0.03	43.1%	223.9
#5	0	56	55 ± 3	79 ± 4	3.3 ± 0.2	1.8 ± 0.3	44.5%	390.8
#6	0.5	0	58 ± 3	91 ± 10	3.25 ± 0.09	3.08 ± 0.03	5.5%	N/A
#7	0.5	0	56 ± 4	90 ± 4	3.23 ± 0.03	3.07 ± 0.01	5.0%	N/A
#8	1	0	78 ± 6	213 ± 6	3.09 ± 0.06	2.70 ± 0.04	12.7%	N/A
#9	0.5	42	86 ± 4	141 ± 9	3.28 ± 0.12	2.09 ± 0.03	36.3%	133.2

[a] Average values of fouling fluids obtained at both the inlet and outlet of PHE at three different running time and one from the launching tank.
[b] Average values of fouling fluids obtained at the inlet of PHE at three different running time and one from the launching tank.
[c] Average values of fouling fluids obtained at the outlet of PHE at three different running time.
[d] BLG denaturation level = 1-$[BLG]_{outlet}$/$[BLG]_{inlet}$.
[e] N/A: the fouling mass is undetectable.

introduced by casein, no detectable fouling was obtained for fouling solutions without adding CaCl₂ (even up to Casein/WPI at 1). Besides that, a low BLG denaturation level was also observed in these cases, suggesting only few BLG molecules denatured during the thermal treatment within PHE. These results might due to the capacity of casein to reduce the ionic calcium at higher temperatures (Broyard and Gaucheron, 2015; Dalgleish and Corredig, 2012; On-Nom et al., 2010). Hence, even though the solutions contained high level of Ca^{2+} (measured at 25 °C), the amount of Ca^{2+} could be reduced to the level that might not be sufficient enough to induce significant denaturation of BLG and subsequent fouling. The results of Fluid#9 confirm this idea by adding 42 ppm Ca^{2+} into fouling solution containing 0.5 wt% WPI and 0.25 wt% casein (*i.e.* Fluid#6 and #7). This solution induced 133.2 g of dried fouling deposit with 36.3% of denatured BLG inside PHE.

3.2. The effect of casein on fouling deposit mass

As shown in the last section, additional Ca^{2+} is required to observe significant fouling. Consequently, in order to investigate the effect of casein on the fouling mass, it was decided to add a constant amount of Ca^{2+} (*i.e.* 42 ppm) for all the fouling solutions containing casein. The calcium content of twelve fouling fluids composed of elevated casein concentration with supplemented 42 ppm Ca^{2+} and their fouling results are displayed in Table 3.

A clear view of how casein affects the fouling can be seen in Fig. 4(a): at Casein/WPI lower than 0.2, fouling mass drop dramatically as Casein/WPI increases, leading to a minimum mass of 42.3 g and that is almost 80% reduction compared to that without casein. Exceeding Casein/WPI of 0.2, the fouling mass increases gradually as Casein/WPI goes higher. More detailed information about fouling mass in each PHE pass is presented in Fig. 4(b). In general, fouling mass increases along the PHE with maximum values at the last pass. Similar fouling starting points were found to be located between 4th and 5th pass, where the temperature ranges from 71.6 to 73.7 °C. These values are in accordance with the denaturation temperature of BLG at 72 °C (Boye and Alli, 2000). One exception can be observed at Casein/WPI of 0.2 (Fluid #7) where apparent fouling (>1 g) can only be found at the 7th pass with an average temperature at 79 °C. The surface coverage of fouling deposit inside PHE can be calculated using the area between the 4th and 10th pass of PHE as shown in Fig. S4. Without adding casein, the fouling mass coverage is ~215 g/m², corresponding to a mean fouling rate at 1.8 g/(m²·min). This fouling rate is comparable to the other large scale fouling experiments with similar PHE configurations using 1 wt% WPC (whey protein concentrate) fouling fluid at a calcium concentration of ~70 mg/L (Khaldi et al., 2015). Surprisingly, the minimum fouling rate

observed at Casein/WPI of 0.2 is close to that obtained for milk fouling in pasteurization studies, *e.g.* between 150 and 250 mg/(m²·min) (Barish and Goddard, 2013; Choi et al., 2013).

Pressure-drop and thermal resistance (*Rf*) are usually employed to monitor fouling within PHE systems. On one hand, fouling causes the hydraulic diameter to decrease during operating, arising the pressure-drop over time until the system collapses. On the other hand, due to the low heat conductivity of the deposits, the additional fouling layer hinders the heat transfer between the hot water and the processing fluid. Fig. 5(a) and (b) show the pressure-drop and thermal resistance (*Rf*) evolutions of fouling runs processed at various Casein/WPI ratios, respectively. The pressure-drop changes little at the first operating hour for all solutions and increase dramatically thereafter. While for *Rf*, the values keep increasing as fouling growing during the whole process. Similar trend can be observed for the maximum values of pressure-drop and *Rf* (*i.e.* values obtained at the end of fouling run), which both of them decrease as Casein/WPI increases, reaching minimum values at Casein/WPI of 0.2. This is consistent with the fouling mass behavior. Worthy noticing is that, at Casein/WPI≥0.2, the extent of increased *Rf* resembles that of total fouling mass, while the increased pressure-drop is less significant. This is confirmed by plotting normalized values of fouling mass and maximum values of pressure-drop and *Rf* against Casein/WPI as shown in Fig. 6. At Casein/WPI>0.2, high fouling mass can be obtained but induce much less pressure-drop (six times lower). This could be attributed to a different fouling structure formed at Casein/WPI>0.2.

It has long been recognized that caseins have chaperone-like functions on the thermal denaturation or aggregation of whey proteins (Wijayanti et al., 2014; Yong and Foegeding, 2010). For instance, κ-casein is the most frequently mentioned one in the literature that can interact with denatured BLG molecule through SH/SS interchange reaction and also hydrophobic interactions (Haque and Kinsella, 2009; Jang and Swaisgood, 1990). These interactions were proposed to terminate the SH/SS exchanges between denatured BLG and thus act as a dead-end reaction for the propagation of BLG aggregation (Donato and Guyomarc'h, 2009). On the other hand, the chaperone behavior of α and β-casein has also been revealed to suppress the thermal denaturation of whey proteins or other unrelated proteins, such as insulin, alcohol dehydrogenase probably through hydrophobic interactions (Bhattacharyya and Das, 1999; Morgan et al., 2005). Consequently, we can expect that the fouling mass should be positively correlated to the BLG denaturation level. Nevertheless, our results do not really support the hypothesis and seem to indicate that BLG denaturation level is not a pertinent indicator to rank fouling behavior for casein-based protein solutions (Fig. S5). Indeed, significant different fouling mass was

Table 3
Calcium content of twelve fouling fluids and their fouling results. For each fouling experiment, the BLG concentration at the inlet and outlet of PHE are also shown. Errors represent standard deviation (SD). Note all solutions contain 42 ppm additional Ca^{2+}.

Fluid#[a]	Casein/WPI	$[Ca]_f$[b] (ppm)	$[Ca]_t$[b] (ppm)	$[BLG]_{inlet}$[c] (g/L)	$[BLG]_{outlet}$[d] (g/L)	BLG denaturation level[e]	Total fouling mass (g)
#1	0	53.0 ± 1.9	64.7 ± 2.6	3.28 ± 0.06	1.87 ± 0.03	43.1%	223.9
#2	0.05	53 ± 5	74 ± 2	3.37 ± 0.08	1.90 ± 0.12	43.4%	123.6
#3	0.05	56 ± 5	71 ± 1.1	3.36 ± 0.07	1.83 ± 0.06	45.6%	112.4
#4	0.1	61 ± 3	84 ± 5	3.33 ± 0.08	1.88 ± 0.17	43.6%	130.7
#5	0.15	66.5 ± 1.7	89 ± 6	3.26 ± 0.05	1.95 ± 0.06	40.2%	116.7
#6	0.15	72 ± 4	92 ± 7	3.17 ± 0.05	1.98 ± 0.18	37.7%	146.3
#7	0.2	71 ± 3	91 ± 3	3.24 ± 0.04	2.23 ± 0.01	31.1%	42.3
#8	0.2	68 ± 4	113 ± 3	3.15 ± 0.03	1.82 ± 0.01	42.3%	89.9
#9	0.3	77 ± 3	107 ± 2	3.29 ± 0.04	2.1 ± 0.11	36.0%	85.9
#10	0.5	86 ± 4	141 ± 9	3.28 ± 0.12	2.09 ± 0.03	36.3%	133.2
#11	0.6	93 ± 4	165 ± 5	3.15 ± 0.11	2.04 ± 0.07	35.1%	164.4
#12	0.8	96 ± 9	203 ± 6	3.31 ± 0.07	2.21 ± 0.06	33.3%	185.9

[a] All fouling fluids contain additional 42 ppm Ca^{2+} (in the form of CaCl₂).
[b] Average values of fouling fluids obtained at both the inlet and outlet of PHE at three different running time and one from the launching tank.
[c] Average values of fouling fluids obtained at the inlet of PHE at three different running time and one from the launching tank.
[d] Average values of fouling fluids obtained at the outlet of PHE at three different running time.
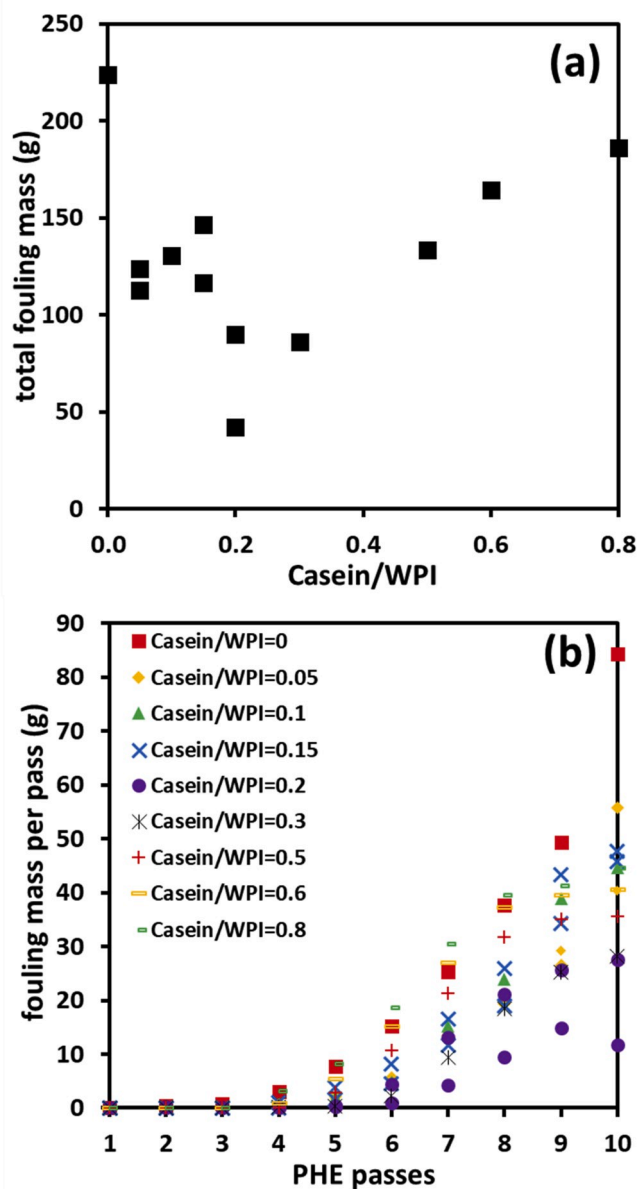[e] BLG denaturation level = 1-$[BLG]_{outlet}$/$[BLG]_{inlet}$.

Fig. 4. (a) Effect of Casein/WPI on the total fouling mass inside PHE. (b) Fouling mass distribution in each pass along the PHE at various Casein/WPI ratios. Note that replicated data at Casein/WPI of 0.05, 0.15 and 0.2 were obtained from individual experiments.

obtained despite not significantly different values of BLG denaturation level (Fluid#1 compare with Fluid#2 to#12, Table 3). Besides, it is observed that the reduction of fouling mass is not accompanied by less denatured BLG proteins (Fluid#1 to#5, Table 3). On the other hand, the BLG denaturation level is significantly lower at higher Casein/WPI (Fluid#9 to#12, Table 3, although in those conditions more fouling mass was observed.

These facts lead us to conclude that it is hard to correlate the BLG denaturation activity with fouling mass behavior. Thereby, a more systematic study on how casein affects the thermal denaturation kinetics of BLG will be discussed in the following section.

3.3. BLG thermal denaturation kinetics

As mentioned previously, we have observed through heat treatment process within PHE that the denaturation level of BLG is almost unchanged when casein was added to WPI protein (Casein/WPI from 0 to
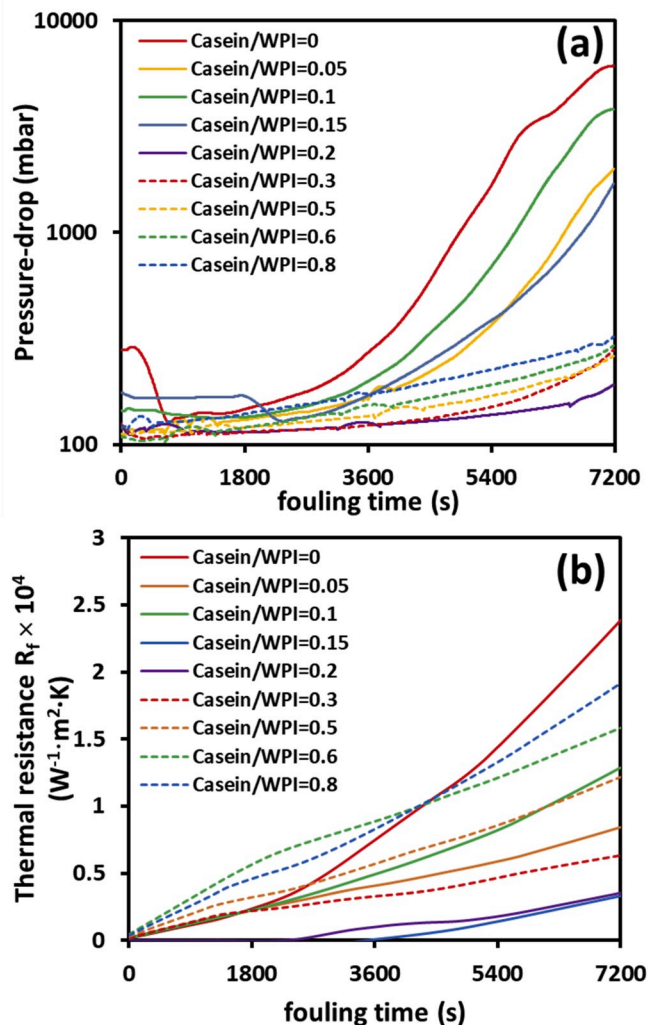

Fig. 5. (a) Pressure-drop and (b) thermal resistance R_f evolution of fouling fluids containing different Casein/WPI within 2 h fouling run. Data at Casein/WPI of 0.05, 0.15 and 0.2 are the average values obtained from two individual experiments. Solid lines represent the results at Casein/WPI≤0.2 and dotted lines refer to that Casein/WPI>0.2. Note that log scale on y-axis on (a).

0.2). Nevertheless, simultaneously a decreasing fouling behavior is observed regarding fouling deposit mass. In order to provide a more exhaustive view on how casein affects the thermal denaturation process of BLG at different temperatures, the thermal denaturation kinetics of BLG were studied at molecular level, using trials at laboratory scale and samples having the same compositions as the fouling fluids applied in the pilot-scale PHE (compositions are shown in Table 1).

Fig. 7(a) is a typical example of the soluble BLG concentration (C_s) evolution with time for a 0.5 wt% WPI solution heat-treated at different holding temperatures (70 °C–90 °C). For a given holding temperature, as expected, C_s decrease with time and for a fixed heating time, C_s decrease sharper with higher holding temperatures. For all the studied conditions, a value of 2 for the reaction order was found to be appropriate. In the literature, the findings for the reaction order for the heat-induced denaturation of BLG commonly varied between 1.5 and 2. For example, several researchers have reported a reaction order of 1.5 (Anema and McKenna, 1996; Dannenberg and Kessler, 1988; Oldfield et al., 1998, 2005), whereas (Hillier and Lyster (1979); Lyster (1970); Manji and Kakuda (1986); Park and Lund (1984)) found that BLG denaturation followed second-order reaction kinetics. This discrepancy among these studies may be explained by the variability of the medium
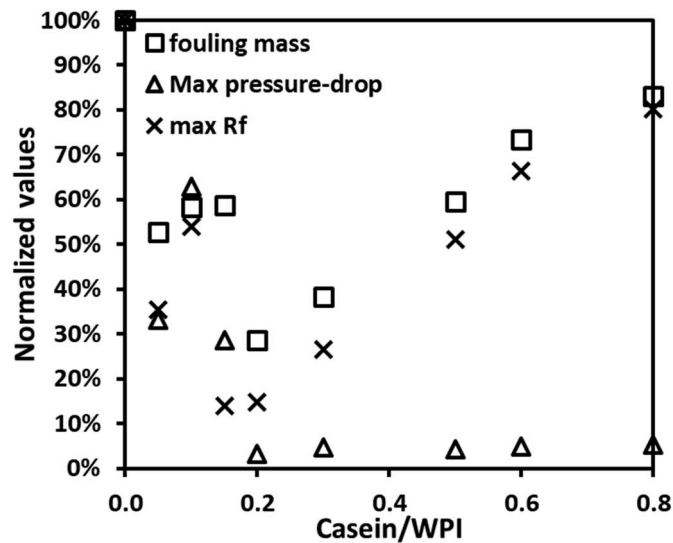
Fig. 6. Effect of Casein/WPI on the normalized total fouling mass and maximum values of pressure-drop and thermal resistance R_f. Notice that the data at Casein/WPI of 0.05, 0.15 and 0.2 are the average values obtained from two individual experiments. Values arc normalized by dividing values obtained at Casein/WPI of 0.

of the protein solution (different buffers or simulated milk ultrafiltrate), the heating treatments (direct stream injection or sealed capillary tubes), protein compositions (isolated BLG or whey with or without casein), protein assays or even statistical approaches (Jaskulka et al., 2000).

Giving the best-fit values of k_f, the logarithm can be plotted against the inverse of the holding temperature in the Arrhenius plot as shown in Fig. 7(b). Analysis of Fig. 7(b) shows clearly that, the introduction of both ionic calcium and micellar casein modifies the denaturation rate constant of BLG while maintaining the same shape (broken slope). Inspection of model solutions containing different Casein/WPI ratios reveals a global increase of k_f when Casein/WPI goes up. The positive shift observed in the ordinate axis in Arrhenius plot appears very moderate for Casein/WPI varying from 0 to 0.2, while at high Casein/WPI such as 0.8, the increase of k_f is more remarkable. More precisely, for Casein/WPI ranges from 0 to 0.2 (corresponding to fouling mass decreasing region), increasing Casein/WPI enhances slightly the BLG denaturation constants for the unfolding step, while in the aggregation limited region, the values are overlapping, suggesting a limited effect of casein on the BLG aggregation process. It is difficult to compare our results with those of literature as in this field few kinetic data of dairy solutions exist. Nevertheless, the significant increase of k_f with higher casein content agrees with those reported in Kessler and Beyer (1991), who found increased denaturation constants at elevated casein/whey proportions from sweet whey to skim milk.

Table 4 is another view of the BLG denaturation behavior in the presence of micellar casein, as it summarizes the corresponding activation energies Ea in each denaturation step calculated from the linear regression in the Arrhenius plot. The calculated Ea for unfolding and aggregation for whey protein solutions are 252 and 210 kJ mol^{-1}, respectively. Note that there is no statistical difference between these two values, indicating there is only one dominant reaction at this temperature range, which is unfolding (70–90 °C). These present Ea are comparable to the range of Ea values in skim milk, 265–280 kJ mol^{-1}, reported by (Anema and McKenna (1996); Dannenberg and Kessler (1988); Oldfield et al. (1998)) for temperature lower than 90 °C. The addition of Ca^{2+} resulted in similar values of aggregation Ea at 230 kJ mol^{-1} to the whey protein but a much larger value of 411 kJ mol^{-1} was found for the unfolding Ea. Similar Ea values have been reported for a 0.5 wt% whey protein with an additional 80 ppm Ca^{2+} (Khaldi et al.,
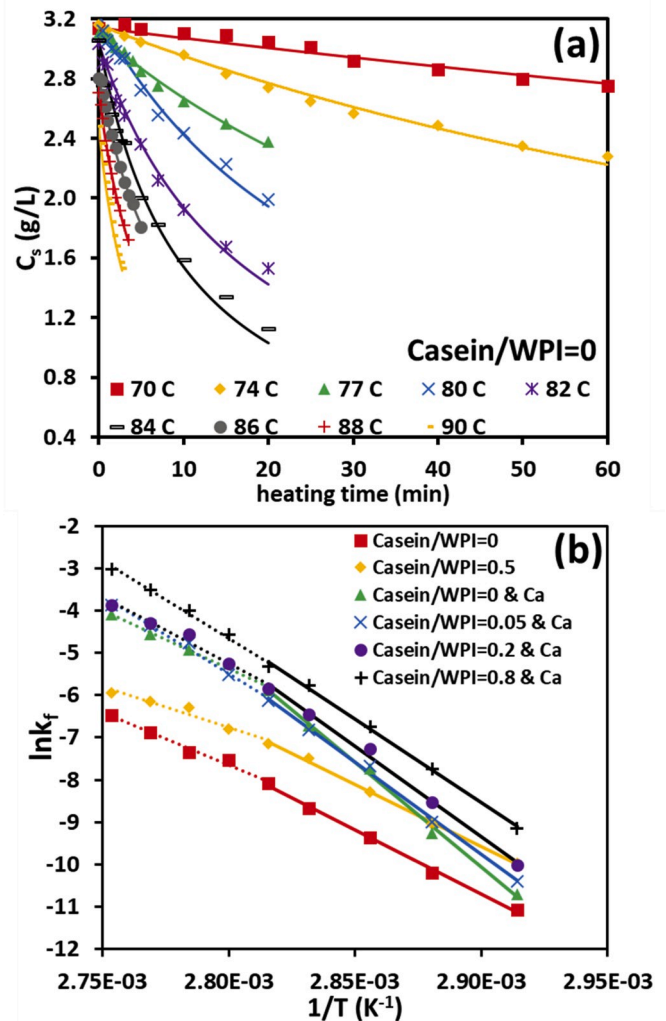

Fig. 7. (a) Evolution of soluble BLG concentration against heating time at various heating temperatures (denote in legend). The solution contains only 0.5 wt% WPI without additional Ca^{2+} (nor casein powder). Solid lines represent best-fit to equation (1) using a reaction order of 2. (b) Arrhenius plot for the BLG denaturation reaction at different protein compositions (shown in Table 1). Solid lines correspond to the linear regressions in the unfolding region while dashed lines refer to the aggregation region.

2018). These results confirm the opposite binary effect of Ca^{2+} on the BLG unfolding step observed by Petit et al. (2011): on one hand, Ca^{2+} facilitates the BLG unfolding by increasing k_f, while on the other hand, Ca^{2+} limits the process by resulting in larger activation energy.

When analyzing more intimately Table 4 for Casein/WPI solutions (varying from 0 to 0.2), increasing Casein/WPI slightly decreases the activation energy for BLG unfolding. From the thermodynamical point of view, it can be assessed that in the presence of abundant ionic calcium, micellar casein does not represent an obstacle to limit the BLG unfolding. On the contrary, the presence of casein does not seem to strongly affect the activation energy for the aggregation process: a clear trend showing decrease or increase is not obtained for the range of Casein/WPI ratio investigated.

To sum up, from Fig. 7 and Table 4, it appears again that the decreased fouling mass at Casein/WPI from 0 to 0.2 is unlikely to be linked to the minor changes in the BLG denaturation reaction due to introduction of casein. It is more probably due to the change in mineral interactions introduced by casein that affects the origin of fouling build-up. For high Casein/WPI (*e.g.* 0.8), the increase of denaturation of BLG is more significant and this time it is possible that the increase of the

Table 4
Calculated kinetic parameters for BLG denaturation at various Casein/WPI using one-step reaction model. Errors denote standard errors from linear regression.

		Casein/WPI ratios							
	Denaturation parameters	0	0.5	0[a]	0.05[a]	0.2[a]	0.8[a]	4[b]	0[c]
Unfolding	$\ln(k^0_{unf})$	77 ± 3	75.5 ± 1.9	133 ± 5	117 ± 4	114 ± 5	105 ± 3	91.0 ± 10.5	141.8
	Ea_{unf} (kJ/mol)	252 ± 9	243 ± 6	411 ± 13	363 ± 11	354 ± 14	327 ± 9	285.5 ± 30.8	431.6
Aggregation	$\ln(k^0_{agg})$	62 ± 5	47 ± 7	72 ± 5	97 ± 6	83 ± 7	98 ± 6	58.8 ± 5.7	74.1
	Ea_{agg} (kJ/mol)	210 ± 15	160 ± 20	230 ± 15	305 ± 18	260 ± 20	303 ± 16	15.3 ± 1.8	233.5

[a] Solutions contain additional 42 ppm Ca^{2+}.
[b] Kinetic data for skim milk reported by Oldfield et al. (1998), while the unfolding region was recognized between 70 and 90 °C.
[c] Kinetic data for whey proteins reported by Khaldi et al. (2018). Solution contained additional 80 ppm Ca^{2+}.

fouling mass is correlated to an increase of BLG denaturation reaction. This is expected as BLG has a larger opportunity to interact with dissociated casein proteins or κ-casein located at the surface of casein micelle, facilitating the aggregation process (Anema and Li, 2003).

3.4. Element mapping of fouling deposit

In order to further investigate the effect of casein on the fouling, the morphology and chemical composition of the fouling layer was characterized using EPMA. For each fouling experiment, the deposits were collected from two different plates (*i.e.* P_{14} and P_{21}) so as to see the influence of temperature on the build-up of the fouling layer. In each EPMA analysis, Fe (iron), S (sulfur), P (phosphate) and Ca (calcium) were determined in the same area of fouling layer cross-section.

Fig. 8 shows the element mapping results of fouling layers obtained from fouling solutions at four different Casein/WPI ratios collected from P_{14}. Repartition of Ca, P and the characteristic element of the protein (S) of the deposit formed at an average temperature of 78.9 °C without the addition of casein is shown in Fig. 8(a). A compact fouling structure was found in this case with homogenously distributed signals of both Ca and S. The P element inside deposit, however, was negligible as the signal in the deposit is even weaker than the stainless steel substrate. This low P signal can be also found in the fouling deposit formed at low casein concentration (Casein/WPI ≤0.2) or at a higher temperature (84.6 °C,

Fig. S6). Moreover, the areas corresponding to Ca and S overlap each other, indicating a co-location of Ca and proteins inside the fouling layer. These results support the idea that in absence of casein and for the range of calcium/BLG ratio investigated (~9), Ca^{2+} acts as binding agents of denatured proteins to co-precipitate upon the hot stainless steel surface (Visser and Jeurnink, 1997). The effect of calcium on the morphology of the fouling layer has been previously reported by Khaldi et al. (2018). These authors demonstrated that the fouling growth mechanism depends and evolve on the increase of Ca/BLG ratios: at low Ca/BLG ratio (2.3), the fouling layer is compact, while in the case of higher Ca/BLG ratio such as 22.9, calcium-based particles act as anchor-points for an arborescent fouling growth.

When casein was present as shown in Fig. 8(b)–(c), heterogenous fouling structures were obtained. In these conditions, the fouling layer was less compact and airier. Moreover, both Ca and S started to be unevenly distributed inside the fouling layer with less intensity of Ca, even though more Ca was present in the fouling fluids (scale bars for each element are identical). Despite this, co-location of Ca and S signals was still apparent in the deposit except at Casein/WPI of 0.8 where P element could no longer be ignored in the fouling layer.

To obtain a deeper insight into the distribution of mineral (Ca, P) in the fouling layer and their interactions with protein (S), overlapped areas of Ca, P and S have been plotted in Fig. 9. It is evidenced that protein favored two types of organization with mineral: either with Ca
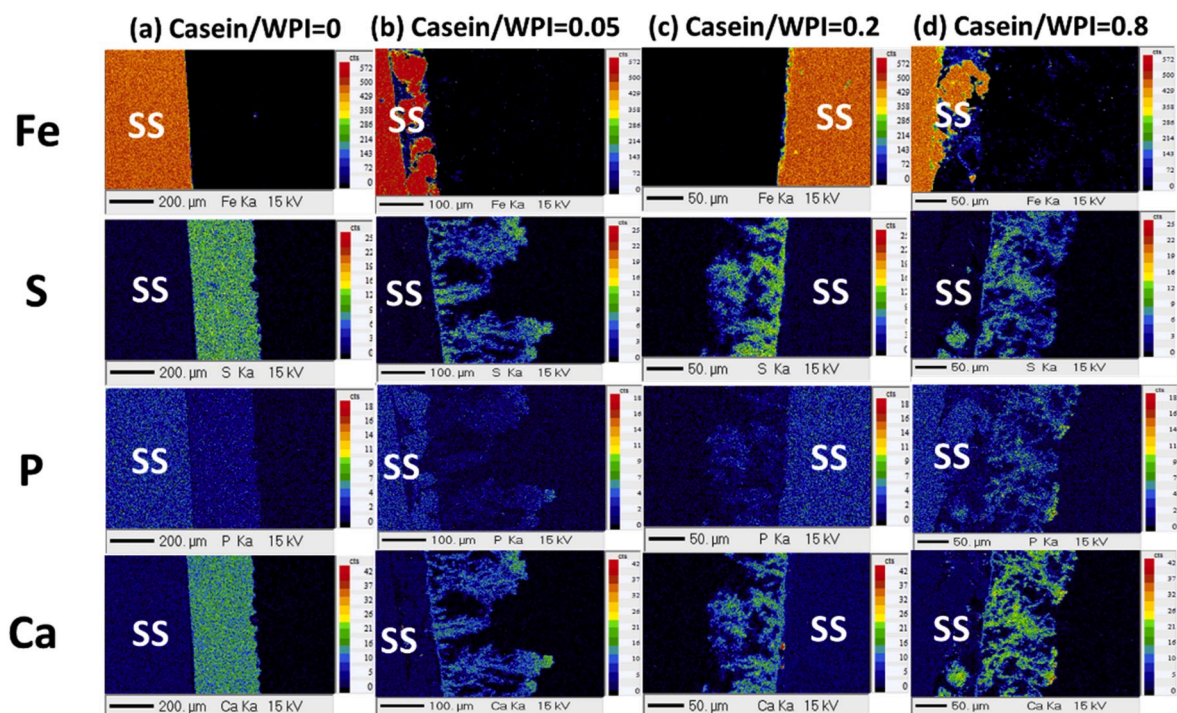

Fig. 8. Fe, S, P and Ca mappings of the cross-section of the fouling layer for fouling fluids at various Casein/WPI ratios of (a) 0 (b) 0.05 (c) 0.2 and (d) 0.8. Deposits were collected from plate P14 with an average temperature of 78.9 °C. SS refers to stainless steel.

alone or with Ca–P as the overlapped area of Ca, P and S (Ca–P–S, green area) differs from that for Ca–S (pink area). Besides, Ca–P–S are more conjugated and act like "tree-trunk" while the Ca–S areas are more scattered around the Ca–P–S. This finding reveals the existence of CaP nanoclusters as Casein/WPI ratio progressively increases, acting as linking agents for fouling build-up. These CaP nanoparticles can be created in the bulk or more possibly introduced from amorphous CaP inside casein micelle (Holt et al., 2013). From this point of view, the increased amount of fouling mass at Casein/WPI from 0.2 to 0.8 could be due to the increased amount of binding agents (CaP). When temperature was higher as shown in Fig. 9(b), the area representing Ca–P–S was relatively smaller but the general trend of CaP surrounding with proteins is consistent. This difference with observation at lower temperature might be caused by the lower level of Ca^{2+} in the bulk (transferred into casein-bound calcium) as Ca^{2+} might also contribute to the formation of CaP nanoclusters.

3.5. SDS-PAGE

To further characterize the fouling deposits, they were analyzed using SDS-PAGE to study the protein composition. Fig. 10 presents the electrophoresis results of eight different fouling deposits formed at four Casein/WPI ratios and collected from two different fouling locations. Pure protein standards were also performed to provide better identification of each protein in the fouling deposits. Results show all fouling deposits are mainly composed of α-casein, β-casein, BLG, and α-la, which is in agreement with those reported for milk fouling (Changani et al., 1997; Jeurnink, 1991). Note that there are few caseins detected even in the condition where casein was not supposed to be present (Casein/WPI of 0). This is probably due to powder elaboration and the difficulty to obtain WPI solutions free of casein during membrane separation process of dairy fractions.

Inspection of casein content in fouling deposits shows a general trend of an increased amount of both α and β-casein in the deposits with higher Casein/WPI ratios. On the other hand, BLG shows similar content inside the deposits for all conditions applied except a significant larger band referring BLG was found for deposits collected from P_{14} at Casein/WPI of 0. Notice that all the fouling deposits were wholly dissolved prior to SDS-PAGE, hence, these results suggest a more proteinaceous deposit formed at a relatively lower temperature with the fouling solution without the addition of casein powder. On the contrary, a more mineral deposit was formed using the same fouling fluid but at a higher temperature condition (*i.e.* P_{21}) as less BLG content was found despite a larger total fouling mass. Notice that the amount of total calcium content for these model fouling fluids is much lower compared to that of normal milk. At this low calcium level, the structure of casein micelle was proposed to swell and individual caseins such as α or β-casein located at

the interior of micelle become easier to dissociate into the bulk. Hence, the increased total fouling mass at Casein/WPI from 0.2 to 0.8 might due to the larger participation of α/β-casein or submicelles in the formation of fouling. The absence of κ-casein in the deposit supports the idea that κ-casein prevents BLG from depositing by formation of κ-casein/BLG complexes in the serum phase (Jeurnink and Dekruif, 1995).

4. Conclusions

In this paper, whey protein-based model solutions containing various Casein/WPI ratios were applied in order to study the effect of casein on the fouling behaviors in a pilot-scale PHE applying a pasteurization schedule. It was firstly established that for the WPI powder used, the ionic calcium was a vital element promoting denaturation and fouling mass deposit. Secondly, for the casein-based protein solutions elaborated, the fouling mass dropped dramatically until a minimum value as Casein/WPI increased to 0.2. However, exceeding this critical Casein/WPI ratio, fouling mass increased with elevated Casein/WPI ratios. Casein/WPI ratio also alters the fouling structure: the fouling layer was compact and homogeneous with evenly distributed calcium and proteins when casein was absent, suggesting a binding role of Ca^{2+} between denatured proteins during the build-up of fouling. However, fouling deposits became heterogeneous and less dense: co-located Ca–S elements were scattered around the Ca–P conjugates. This inhomogeneity suggests that CaP nanoclusters, introduced by micellar casein, may act as new linking species between proteins as the fouling grows.

Results from gel electrophoresis revealed a larger participation of α/β-casein in the fouling deposits at higher Casein/WPI conditions. This might explain why fouling mass increased at high Casein/WPI ratios as more dissociated caseins were involved in the formation of fouling. Concerning BLG denaturation, casein seems poorly affect the BLG denaturation process, and it was shown that the fouling behavior was not correlated to the BLG denaturation level at the conditions where fouling mass decreased (Casein/WPI≤0.2) or increased (Casein/WPI>0.2).

It is finally proposed that micellar casein change deeply the calcium balance and the content of CaP nanocluster modifies sharply the interactions which occur between proteins species (BLG, caseins) and mineral element (ionic calcium, Ca–P) thereby affecting the protein denaturation and mineral precipitation.

CRediT authorship contribution statement

Weiji Liu: Conceptualization, Methodology, Investigation, Validation, Writing - original draft. **Xiao Dong Chen:** Supervision, Project administration, Funding acquisition, Writing - review & editing. **Romain Jeantet:** Writing - review & editing, Visualization, Project
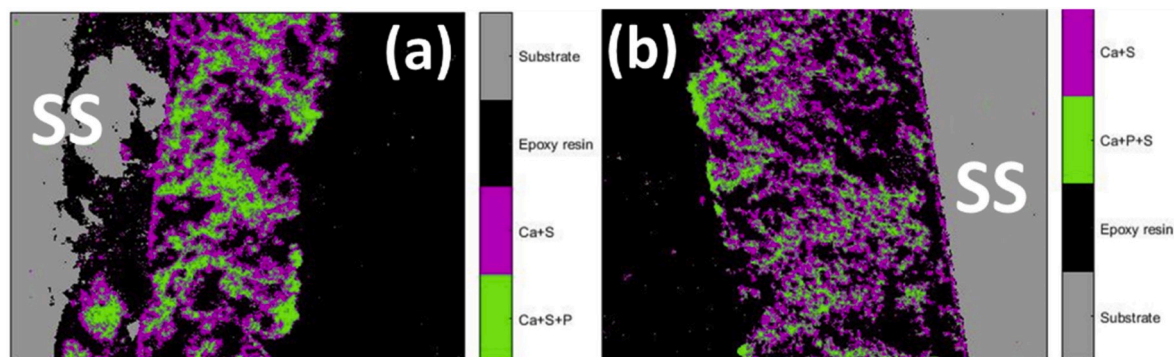
Fig. 9. Overlapped areas of Fe, S, P and Ca elements of the cross-section of the fouling layer. The deposits were collected from the same fouling run using fouling fluid at Casein/WPI of 0.8 but different plates: (a) P_{14} and (b) P_{21} resulting in different fouling temperatures at 78.9 and 84.6 °C, respectively. SS refers to stainless steel. The grey area denotes the SS substrate and the black area refers to the epoxy resin. The area in green corresponds to overlapped signals of Ca, S and P, while the pink area refers to the overlapped Ca and S. (For interpretation of the references to color in this figure legend, the reader is referred to the Web version of this article.)
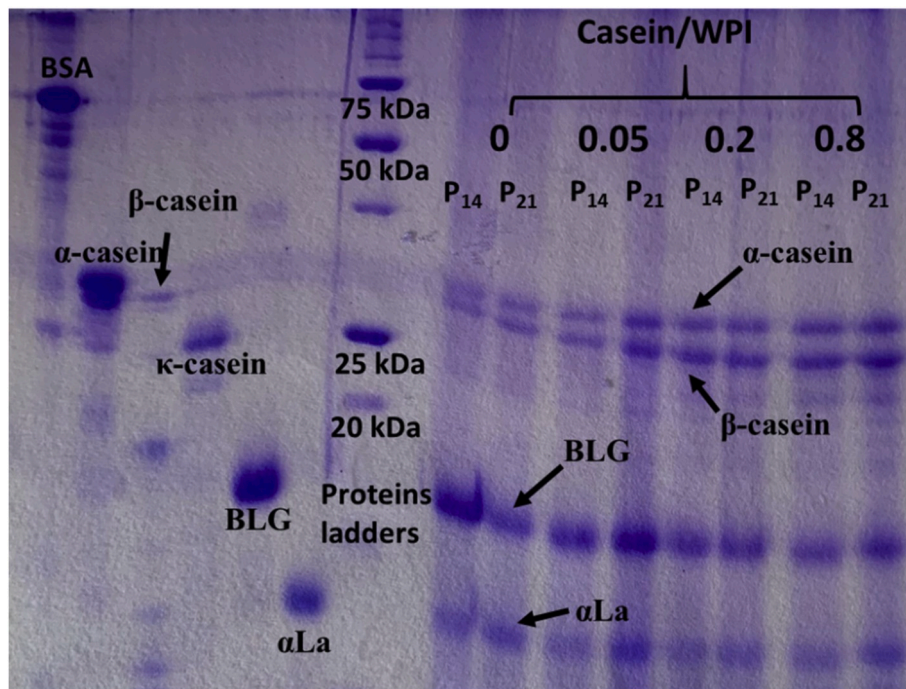
Fig. 10. SDS-PAGE results including pure protein standards, protein ladders, and fouling deposits. Pure proteins are (from left to right) BSA, α-casein, β-casein, κ-casein, BLG, and α-lactalbumin (αLa). Fouling deposits were obtained at different Casein/WPI ratios of 0, 0.05, 0.2 and 0.8; in each condition, deposits were collected from two different plates (P$_{14}$ and P$_{21}$).

administration. **Christophe André:** Supervision, Software, Writing - review & editing, Project administration. **Severine Bellayer:** Investigation. **Guillaume Delaplace:** Conceptualization, Resources, Writing - review & editing, Supervision, Project administration.

Appendix A. Supplementary data

Supplementary data to this article can be found online at https://doi.org/10.1016/j.jfoodeng.2020.110175.

Conflict of interest form

- All authors have participated in (a) conception and design, or analysis and interpretation of the data; (b) drafting the article or revising it critically for important intellectual content; and (c) approval of the final version.
- This manuscript has not been submitted to, nor is under review at, another journal or other publishing venue.
- The authors have no affiliation with any organization with a direct or indirect financial interest in the subject matter discussed in the manuscript

References

Anema, S.G., Li, Y., 2003. Association of denatured whey proteins with casein micelles in heated reconstituted skim milk and its effect on casein micelle size. J. Dairy Res. 70 (1), 73–83.
Anema, S.G., McKenna, A.B., 1996. Reaction kinetics of thermal denaturation of whey proteins in heated reconstituted whole milk. J. Agric. Food Chem. 44 (2), 422–428.
Bansal, B., Chen, X.D., 2006. A critical review of milk fouling in heat exchangers. Compr. Rev. Food Sci. Food Saf. 5 (2), 27–33.
Barish, J.A., Goddard, J.M., 2013. Anti-fouling surface modified stainless steel for food processing. Food Bioprod. Process. 91 (4), 352–361.
Bhattacharyya, J., Das, K., 1999. Molecular Chaperone-like Properties of an Unfolded Protein (s-Casein).
Blanpain-Avet, P., Andre, C., Khaldi, M., Bouvier, L., Petit, J., Six, T., Jeantet, R., Croguennec, T., Delaplace, G., 2016. Predicting the distribution of whey protein fouling in a plate heat exchanger using the kinetic parameters of the thermal denaturation reaction of beta-lactoglobulin and the bulk temperature profiles. J. Dairy Sci. 99 (12), 9611–9630.
Boye, J.I., Alli, I., 2000. Thermal denaturation of mixtures of α-lactalbumin and β-lactoglobulin: a differential scanning calorimetric study. Food Res. Int. 33 (8), 673–682.
Broyard, C., Gaucheron, F., 2015. Modifications of structures and functions of caseins: a scientific and technological challenge. Dairy Sci. Technol. 95 (6), 831–862.
Changani, S.D., Belmar-Beiny, M.T., Fryer, P.J., 1997. Engineering and chemical factors associated with fouling and cleaning in milk processing. Exp. Therm. Fluid Sci. 14 (4), 392–406.
Choi, W., Jun, S., Nguyen, L.T., Rungraeng, N., Yi, H., Balasubramanian, S., Puri, V.M., Lee, J., 2013. 3-D milk fouling modeling of plate heat exchangers with different surface finishes using computational fluid dynamics codes. J. Food Process. Eng. 36 (4), 439–449.
Dalgleish, D.G., Corredig, M., 2012. The structure of the casein micelle of milk and its changes during processing. Annual Review of Food Science and Technology 3 (1), 449–467.
Dannenberg, F., Kessler, H.G., 1988. Reaction kinetics of the denaturation of whey proteins in milk. J. Food Sci. 53 (1), 258–263.
Donato, L., Guyomarc'h, F., 2009. Formation and properties of the whey protein/κ-casein complexes in heated skim milk — a review. Dairy Sci. Technol. 89 (1), 3–29.
Farrell Jr., H.M., Jimenez-Flores, R., Bleck, G.T., Brown, E.M., Butler, J.E., Creamer, L.K., Hicks, C.L., Hollar, C.M., Ng-Kwai-Hang, K.F., Swaisgood, H.E., 2004. Nomenclature of the proteins of cows' milk—sixth revision. J. Dairy Sci. 87 (6), 1641–1674.
Fryer, P.J., Christian, G.K., Liu, W., 2006. How hygiene happens: physics and chemistry of cleaning. International Journal of Dairy Technology 59 (2), 76–84.
Grijspeerdt, K., Mortier, L., De Block, J., Van Renterghem, R., 2004. Applications of modelling to optimise ultra high temperature milk heat exchangers with respect to fouling. Food Contr. 15 (2), 117–130.

Guérin, R., Ronse, G., Bouvier, L., Debreyne, P., Delaplace, G., 2007. Structure and rate of growth of whey protein deposit from in situ electrical conductivity during fouling in a plate heat exchanger. Chem. Eng. Sci. 62 (7), 1948–1957.

Haque, Z., Kinsella, J.E., 2009. Interaction between heated κ-casein and β-lactoglobulin: predominance of hydrophobic interactions in the initial stages of complex formation. J. Dairy Res. 55 (1), 67–80.

Hillier, R.M., Lyster, R.L.J., 1979. WHEY-PROTEIN denaturation IN heated milk and cheese whey. J. Dairy Res. 46 (1), 95–102.

Holt, C., Carver, J.A., Ecroyd, H., Thorn, D.C., 2013. Invited review: caseins and the casein micelle: their biological functions, structures, and behavior in foods1. J. Dairy Sci. 96 (10), 6127–6146.

Jang, H.D., Swaisgood, H.E., 1990. Disulfide bond formation between thermally denatured β-lactoglobulin and κ-casein in casein micelles. J. Dairy Sci. 73 (4), 900–904.

Jaskulka, F.J., Smith, D.E., Larntz, K., 2000. Determining the kinetic reaction rate order for the thermal denaturation of β-lactoglobulin using two statistical approaches. Int. Dairy J. 10 (9), 589–595.

Jeurnink, T.J.M., 1991. Effect of proteolysis in milk on fouling in. heat-exchangers Netherlands Milk And Dairy Journal 45 (1), 23–32.

Jeurnink, T.J.M., Dekruif, K.G., 1995. Calcium-concentration in milk in relation to heat stability and fouling. Neth. Milk Dairy J. 49 (2–3), 151–165.

Kehoe, J.J., Wang, L., Morris, E.R., Brodkorb, A., 2011. formation of non-native β-lactoglobulin during heat-induced denaturation. Food Biophys. 6 (4), 487.

Kessler, H.-G., Beyer, H.-J., 1991. Thermal denaturation of whey proteins and its effect in dairy technology. Int. J. Biol. Macromol. 13 (3), 165–173.

Khaldi, M., Blanpain-Avet, P., Guérin, R., Ronse, G., Bouvier, L., André, C., Bornaz, S., Croguennec, T., Jeantet, R., Delaplace, G., 2015. Effect of calcium content and flow regime on whey protein fouling and cleaning in a plate heat exchanger. J. Food Eng. 147, 68–78.

Khaldi, M., Croguennec, T., André, C., Ronse, G., Jimenez, M., Bellayer, S., Blanpain-Avet, P., Bouvier, L., Six, T., Bornaz, S., Jeantet, R., Delaplace, G., 2018. Effect of the calcium/protein molar ratio on β-lactoglobulin denaturation kinetics and fouling phenomena. Int. Dairy J. 78, 1–10.

Lewis, M.J., 2011. The measurement and significance of ionic calcium in milk - a review. International Journal of Dairy Technology 64 (1), 1–13.

Lyster, R.L.J., 1970. The denaturation of α-lactalbumin and β-lactoglobulin in heated milk. J. Dairy Res. 37 (2), 233–243.

Mahdi, Y., Mouheb, A., Oufer, L., 2009. A dynamic model for milk fouling in a plate heat exchanger. Appl. Math. Model. 33 (2), 648–662.

Manji, B., Kakuda, Y., 1986. Thermal denaturation of whey proteins in skim milk. Can. Inst. Food Sci. Technol. J. 19 (4), xxxvii.

Miyawaki, A., Sawano, A., Kogure, T., 2003. Lighting up cells: labelling proteins with fluorophores. Nat. Cell Biol. Suppl, S1–S7.

Morgan, P.E., Treweek, T.M., Lindner, R.A., Price, W.E., Carver, J.A., 2005. Casein proteins as molecular chaperones. J. Agric. Food Chem. 53 (7), 2670–2683.

Oldfield, D.J., Singh, H., Taylor, M.W., 2005. Kinetics of heat-induced whey protein denaturation and aggregation in skim milks with adjusted whey protein concentration. J. Dairy Res. 72 (3), 369–378.

Oldfield, D.J., Singh, H., Taylor, M.W., Pearce, K.N., 1998. Kinetics of denaturation and aggregation of whey proteins in skim milk heated in an ultra-high temperature (UHT) pilot plant. Int. Dairy J. 8 (4), 311–318.

On-Nom, N., Grandison, A.S., Lewis, M.J., 2010. Measurement of ionic calcium, pH, and soluble divalent cations in milk at high temperature. J. Dairy Sci. 93 (2), 515–523.

Park, K.H., Lund, D.B., 1984. Calorimetric study of thermal denaturation of β-lactoglobulin. J. Dairy Sci. 67 (8), 1699–1706.

Patocka, G., Jelen, P., Kalab, M., 1993. Thermostability of skimmilk with modified casein/whey protein content. Int. Dairy J. 3 (1), 35–48.

Paulsson, M., Dejmek, P., 1990. Thermal denaturation of whey proteins in mixtures with caseins studied by differential scanning calorimetry. J. Dairy Sci. 73 (3), 590–600.

Petit, J., Herbig, A.L., Moreau, A., Delaplace, G., 2011. Influence of calcium on β-lactoglobulin denaturation kinetics: implications in unfolding and aggregation mechanisms. J. Dairy Sci. 94 (12), 5794–5810.

Petit, J., Six, T., Moreau, A., Ronse, G., Delaplace, G., 2013. β-lactoglobulin denaturation, aggregation, and fouling in a plate heat exchanger: pilot-scale experiments and dimensional analysis. Chem. Eng. Sci. 101, 432–450.

Price, W.V., 1927. Concerning the addition of calcium chloride to milk for cheese making. J. Dairy Sci. 10 (5), 373–376.

Sadeghinezhad, E., Kazi, S.N., Dahari, M., Safaei, M.R., Sadri, R., Badarudin, A., 2015. A comprehensive review of milk fouling on heated surfaces. Crit. Rev. Food Sci. Nutr. 55 (12), 1724–1743.

Sawyer, W.H., Norton, R.S., Nichol, L.W., McKenzie, G.H., 1971. Thermodenaturation of bovine β-lactoglobulin: kinetics and the introduction of β-structure. Biochim. Biophys. Acta Protein Struct. 243 (1), 19–30.

Shimada, K., Cheftel, J.C., 2002. Sulfhydryl group/disulfide bond interchange reactions during heat-induced gelation of whey protein isolate. J. Agric. Food Chem. 37 (1), 161–168.

Tolkach, A., Kulozik, U., 2007. Reaction kinetic pathway of reversible and irreversible thermal denaturation of beta-lactoglobulin. Lait 87 (4–5), 301–315.

Udabage, P., McKinnon, I.R., Augustin, M.-A., 2000. Mineral and casein equilibria in milk: effects of added salts and calcium-chelating agents. J. Dairy Res. 67 (3), 361–370.

Ven Murthy, M.R., Carrier-Malhotra, L., 1989. Progressive unfolding of the conformational states of transfer RNA and ribosomal 5S RNA by methylene blue binding. In: Vijayalakshmi, M.A., Bertrand, O. (Eds.), Protein-Dye Interactions: Developments and Applications. Springer Netherlands, Dordrecht, pp. 316–330.

Visser, J., Jeurnink, T.J.M., 1997. Fouling of heat exchangers in the dairy industry. Exp. Therm. Fluid Sci. 14 (4), 407–424.

Wijayanti, H.B., Bansal, N., Deeth, H.C., 2014. Stability of whey proteins during thermal processing: a review. Compr. Rev. Food Sci. Food Saf. 13 (6), 1235–1251.

Yong, Y.H., Foegeding, E.A., 2010. Caseins: utilizing molecular chaperone properties to control protein aggregation in foods. J. Agric. Food Chem. 58 (2), 685–693.